

Dating of Precambrian Metasedimentary Rocks and Timing of their Metamorphism in the Soursat Metamorphic Complex (NW IRAN): Using LA-ICP-MS, U-Pb Dating of Zircon and Monazite

M. Jamshidi Badr,^{1*} F. Masoudi,^{2,4} A.S. Collins,³ and G. Cox³

¹Department of Geology, Faculty of Sciences, Islamic Azad University, Karaj Branch, Islamic Republic of Iran

²Department of Geology, Faculty of Sciences, Tarbiat Moallem University, Tehran, Islamic Republic of Iran

³Tectonics, Resources and Exploration (TRaX), School of Earth and Environmental Sciences, University of Adelaide, SA 5005, Australia

⁴Department of Geology, Faculty of Sciences, Shahid Beheshti University, Tehran, Islamic Republic of Iran

Received: 13 March 2010 / Revised: 4 August 2010 / Accepted: 24 October 2010

Abstract

Soursat Metamorphic Complex (SMC) in west of Takab city is one of the polyphase metamorphic terranes in northern Sanandaj-Sirjan metamorphic belt of Iran. The SMC composed mainly of metasedimentary rocks associated with granitic intrusions. Based on metamorphic rocks, two metamorphic phases could be separate in the complex. M1 is representative of regional metamorphisms which varies from greenschist to amphibolite facies and consists of mica-schist, garnet-schist, staurolite-schist, kyanite-schist, fibrolite-schist, garnet amphibolites, marble, gneiss. M2 is contact metamorphism with clear outcrop just in the central of SMC and overprinted on M1. This phase consists of andalusite-schist, cordierite-schist and Actinolite-schist. SMC is in tectonic contact with Precambrian to Paleozoic sedimentary rocks which make it difficult to date it based on stratigraphy. In this study, U-Pb dating of zircons and Monazites used in order to find the ages of deposition and metamorphism of metasediments in SMC. U-Pb dating of zircons from a staurolite-schist in the complex by laser ablation inductively coupled plasma mass spectrometry (LA-ICP-MS) yielded a maximum Precambrian depositional age of 605 ± 43 . Monazites were also dated from a garnet-schist using the same technique and yielded a $^{238}\text{U}/^{206}\text{Pb}$ age of 61 ± 8 which is interpreted as the age of the regional metamorphism. Based on these ages, metasedimentary protoliths of the SMC are deposited at the same time as the surrounding essentially unmetamorphosed Precambrian-Cambrian sedimentary rocks and regional metamorphism occurred later in Paleocene and could be related to the orogenesis during the collision of Arabian plate with Iranian block and closure of Neotethys.

Keywords: LA-ICP-MS Dating; Precambrian; Soursat Metamorphic Complex; Takab

Introduction

Sanandaj-Sirjan Zone (SSZ) in Iran is a metamorphic

zone which was exhumed subsequent to collision between accreted the Afro-Arabian continent and the Iranian microcontinent terranes. Subduction of the

* Corresponding author, Tel.: +98(21)88309293, Fax: +98(21)88309293, E-mail: m_jamshidi76@yahoo.com

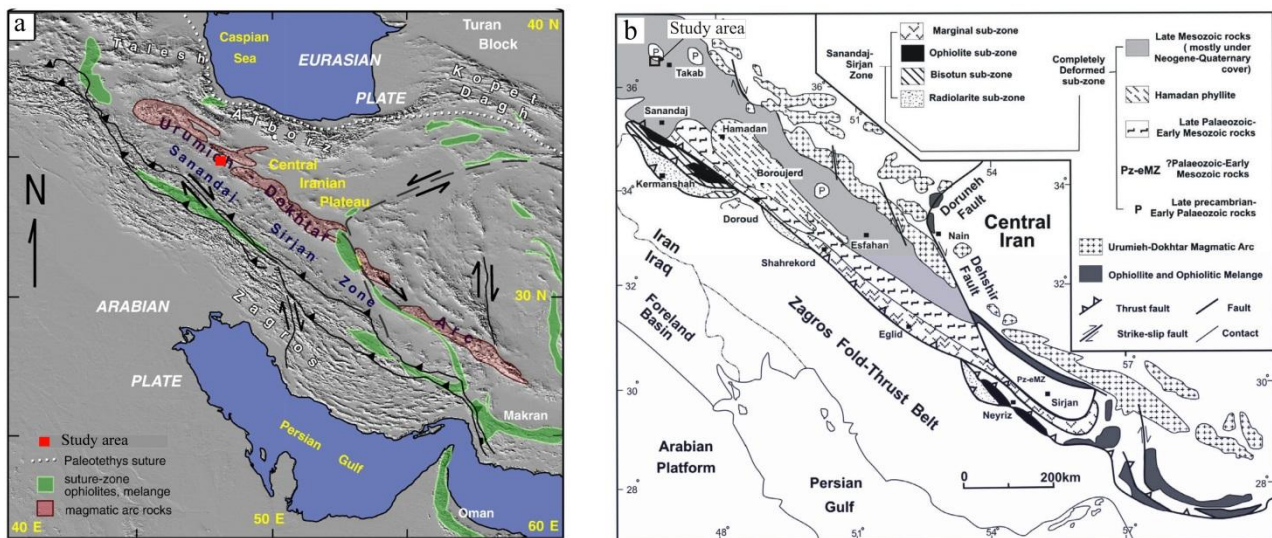


Figure 1. (a) Geologic map of Iran and surrounding regions showing mountain belts, Zagros fold-thrust belt (after [15]). Red square indicates study area (b) Location of the Sanandaj-Sirjan belt in Iran and black square shows the study area (after [35]).

Tethyan sea floor under Central Iran along the Sanandaj-Sirjan Zone initiated prior to the Late Cretaceous/Paleocene [5,30,31,34,35], or about 20 million years, in the latest Eocene [3,4]. Sanandaj-Sirjan zone acting as a deformable backstop [48] and is a region of polyphase deformation which the youngest one recorded the collision [1]. The grade of metamorphism in SSZ is reported to be mainly greenschist and lower to upper amphibolite facies [e.g. 6, 34 and 44]. However, high-pressure metamorphism is also observed [12].

The Soursat Metamorphic Complex (SMC) is one of the polyphase metamorphic terranes in northern Sanandaj-Sirjan Metamorphic belt of Iran (Fig. 1). SMC is in tectonic contact with Precambrian to Paleozoic sedimentary rocks (Kahar, Bayandor, Soltaniyeh, Barut, Lalun and Mila formations) which make it difficult to date it based on stratigraphy. The age of Soursat Complex was first reported in the Shahin Dezh geological map (scale 1:250000) [2], where it was tentatively assigned a Precambrian age (see also [16, 17, 37]) and viewed as analogous to the Precambrian basement rocks exposed in the Arabian shield (e.g., [48]). Previous attempts at dating rocks within the SMC (Pichagchi pluton) have employed the K-Ar technique and yielded an age of ~75 Ma [26]. This age has directly influenced palaeogeographic and plate tectonic reconstructions [27], yet its significance is far from clear. However, the association of granitoids with old basement in SMC, also suggesting that plutonism could

not be entirely related to the events which formed SSZ during Subduction of the Tethyan Sea.

This research is focused on U–Pb Laser Ablation ICP-MS dating of metasedimentary rocks and timing of their metamorphism in the SMC. Modern U–Pb Laser Inductively Coupled Mass Spectrometry (LA-ICP-MS) for zircon is the preferred methods for determining deposition ages of metasedimentary due to the closure temperature of the U–Pb system well in excess of the solidus $700\text{--}750\text{ }^{\circ}\text{C}$ and the refractory nature of zircon and U–Pb Laser Inductively Coupled Mass Spectrometry (LA-ICP-MS) for monazite is the preferred methods for determining metamorphism. The results could apply to constrain the sequence of the events and evolution of northern SSZ.

Materials and Methods

Geological Setting

SMC have been studied since the term was introduced by Pelissier [41] and Darvishzadeh [9], because of the presence of different metamorphic rocks, granitoids and its tectonic settings. Geology of complex reviewed in detail by many researchers (see e.g. [2, 13, 14, 22, 23, 24, 26, 27, 29, 30 and 33]).

SMC formed by metasedimentary, metavolcanosedimentary rocks and associated granitic intrusions. The complex presents tectonic contact with nearby sedimentary rocks. Two main geological units have

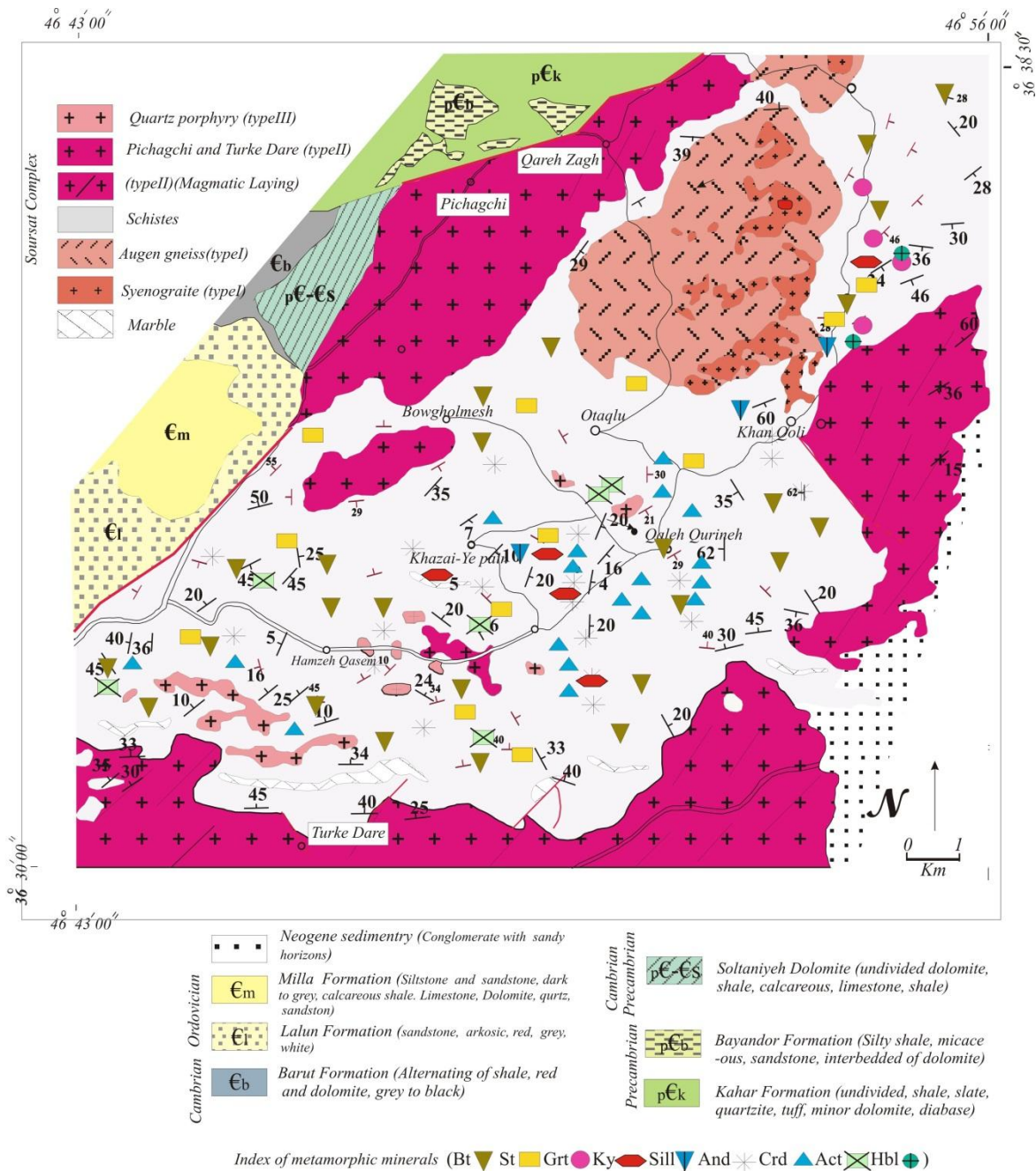


Figure 2. Simplified geological map of the SMC, showing distribution and mineral assemblages of metamorphic rocks and main outcrops of different granitoids.

been described for Precambrian to Paleozoic sedimentary rocks [27]: (1) upper Precambrian Kahar formation consisting of slate, sandstone and some acidic volcanic rocks those locally reveal a very low metamorphic grade, and (2) Precambrian-Cambrian and Ordovician dolomite (Kahar, Bayandor and Soltaniyeh formations), sandstone, shale and dolomitic limestone

(Barut, Lalun and Mila Formations) (Fig. 2).

Metamorphic rocks are mainly mica-schist, garnet-schist, staurolite-schist, kyanite schist, fibrolite schist, andalusite-schist, cordierite-schist, Actinolite schist, marbel, garnet amphibolites, gneiss and granite-gneiss (Fig. 3).

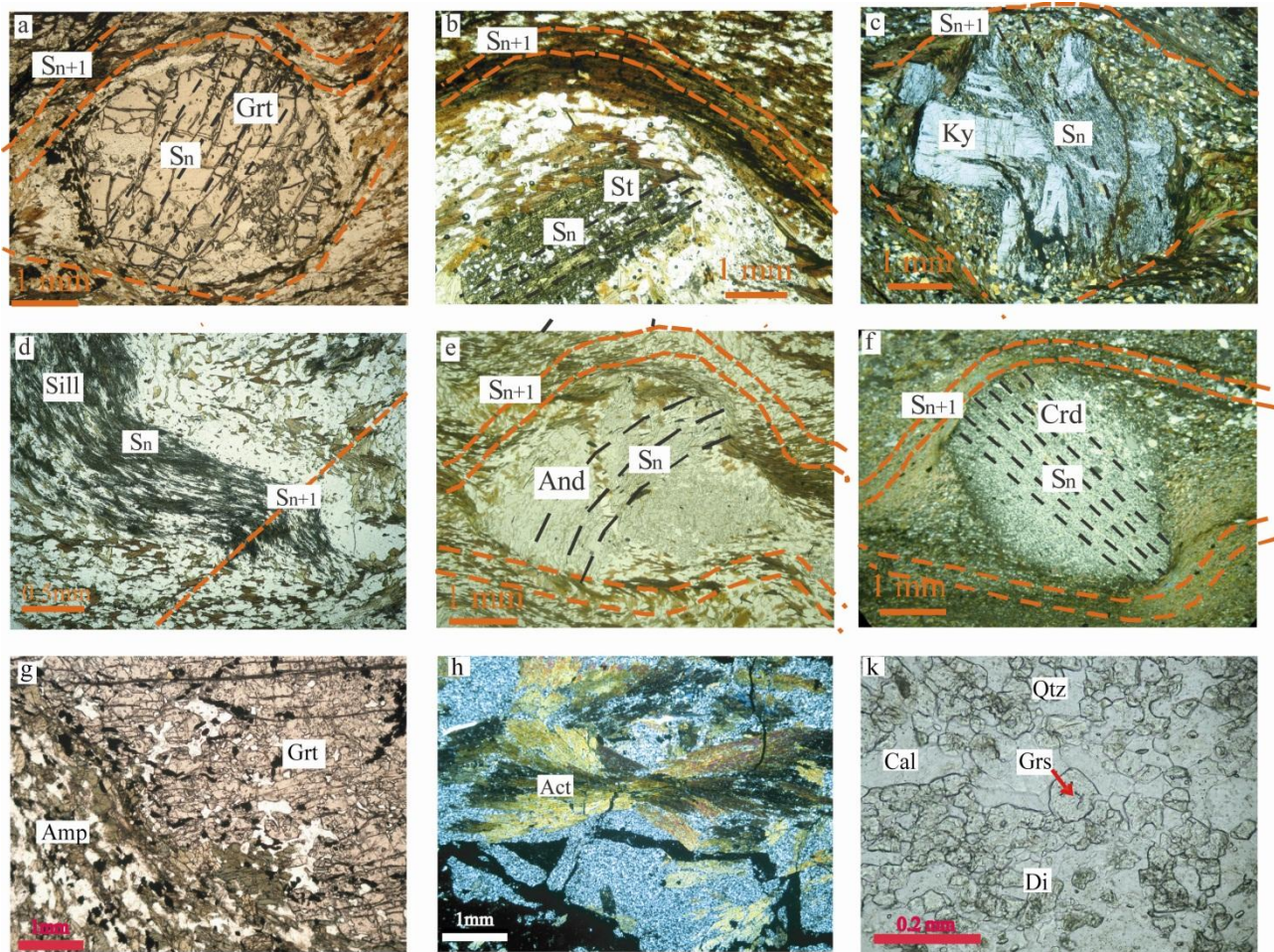


Figure 3. Microphotographs showing different metamorphic rocks and representative textural relationships in metapelites of SMC. a) Garnet porphyroblast with Sn inclusion trails, that is defined by quartz and opaque minerals. Biotite and quartz (Sn) in matrix is crenulated (Fn+1). Crenulations deflect the garnet porphyroblast; b) Staurolite porphyroblast with Sn inclusion trails which defined by quartz and opaque minerals. Muscovite and quartz (Sn) in matrix is crenulated (Fn+1). Crenulations deflect the staurolite porphyroblast; c) Kyanite with Sn inclusion trails which are defined by quartz and opaque minerals and external Crenulations (Sn+1) deflect the internal schistosity (Sn); d) Sillimanite (fibrolite) porphyroblast with Sn inclusion trails that are defined by quartz and opaque minerals. Muscovite and quartz (Sn) in matrix is crenulated (Fn+1); e) Andalusite with Sn inclusion trails that are defined by quartz and opaque minerals and external Crenulations (Sn+1) deflect the internal schistosity (Sn); f) Cordierite porphyroblast with Sn inclusion trails that is defined by quartz, biotite, muscovite and opaque minerals and external Crenulations (Sn+1) deflect the internal schistosity (Sn); g) Photomicrograph of garnet porphyroblast in garnet-bearing amphibolite rock (long dimension up to 6 mm). Garnet contains inclusions of ilmenite and quartz also present in the matrix; h) Actinolite schist with fan type texture that outcrop in central of SMC; k) marble with diopside, grossular, calcite and quartz. (Gr, garnet; St, staurolite; Ky, kyanite; Sill, sillimanite; And, andalusite; crd, cordierite; Am, amphibolite; Act, Actinolite; Grs, grossular; Di, diopside; Cal, calcite; Qtz, quartz).

Laser Ablation ICP-MS Dating

ICP-MS dating of Zircon and monazite crystals in two schists were obtained on University of Adelaide based on following basics. Zircons were separated using conventional methods that include crushing, sieving, magnetic separation and floatation. More than fifty zircon grains were handpicked under a binocular

microscope. The zircons were then set in synthetic resin mounts, polished and cleaned in a warm HNO₃ ultrasonic bath. Cathodoluminescence (CL) and back-scattered electron (BSE) imaging were carried out to help characterize any compositional variation within individual zircons. Equipment and operating conditions for zircon analysis were identical to those reported by Payne *et al.* [40]. A spot size of 30 μm and repetition

rate of 5 Hz was used for U–Pb data acquisition, producing a laser power density of ~8 J/cm². Zircon ages were calculated using the GEMOC GJ-1 zircon standard to correct for U–Pb fractionation (TIMS normalization data ²⁰⁷Pb/²⁰⁶Pb=608.3 Ma, ²⁰⁶Pb/²³⁸U = 600.7 Ma and ²⁰⁷Pb/²³⁵U = 602.2 Ma — [21]), and the GLITTER software for data reduction [50]. Over the duration of this study the reported average normalized ages for GJ-1 were 609±10, 600.2±2.7 and 601.9±2.4 Ma for the ²⁰⁷Pb/²⁰⁶Pb, ²⁰⁶Pb/²³⁸U and ²⁰⁷Pb/²³⁵U ratios, respectively (n=24).

Metamorphic monazite from sample Sh-68 was imaged using backscattered electron imagery (BSE) and conducted by LA-ICPMS at the University of Adelaide. Equipment and operating conditions for monazite analysis are identical to those reported by Payne et al. [39, 40]. U–Pb acquisition utilized 10 µm beam diameter for monazite run at a repetition rate of 5 Hz. Monazite ages were calculated using the MADEL monazite standard to correct for U–Pb fractionation (TIMS normalisation data: ²⁰⁷Pb/²⁰⁶Pb=490.7 Ma, ²⁰⁶Pb/²³⁸U=514.8 Ma, ²⁰⁷Pb/²³⁵U=510.4 Ma: [39]), and again the GLITTER software for data reduction. Over the duration of this study, the reported average normalised ages for MADEL are 493.0+8.3, 514.3+2.4 and 511.2+2.0 Ma for the ²⁰⁷Pb/²⁰⁶Pb, ²⁰⁶Pb/²³⁸U and ²⁰⁷Pb/²³⁵U ratios, respectively (n=32). Accuracy was monitored by repeat analyses of the in-house internal monazite standard (94–222/ Bruna-NW: ²⁰⁶Pb/²³⁸U=447 Ma: [39]). Over the duration of this study, the reported average ²⁰⁶Pb/²³⁸U age for the internal standard was 446.9+3.1 Ma (n=15).

Result and Discussion

Metamorphic Rocks of SMC

Metapelitic rocks in SMC contain garnet, staurolite, kyanite, fibrolite, cordierite and andalusite. Porphyroblasts in schists have the same petrofabric and three schistosity (Sn) inclusion trails are also offset by conjugate sets of extensional schistosity (Sn+1) and (Sn+2) made crenulations on (Sn+1) (Fig. 3). The same texture of cordierite and andalusite with garnet, staurolite, kyanite and fibrolite porphyroblast formed during the same deformation phase and related to regional folding that reported by Ghasemi [13], Jamshidi badr [24] and Masoudi [30] in SMC. However, the minerals aren't paragenesis [24]. Metapelitic rocks in the SMC have previously been separated into the kyanite- and andalusite-types. The kyanite-type involves of biotite, garnet, staurolite, kyanite, Sillimanite which refer to

regional metamorphic (M1) with medium P-T. The andalusite-type includes biotite, cordierite and, locally, Staurolite. Actinolite schists are also present as metabasic rocks and are refer to contact metamorphic phase (M2) with high T-low P [24].

Assemblage of M1 metamorphic phase is present in

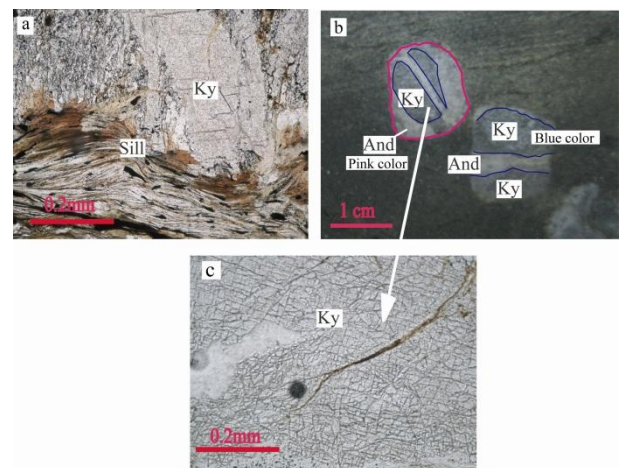


Figure 4. Photographs showing the textural relationships of aluminosilicates in SMC metapelites (PPI). (a) Kyanite porphyroblast with high relief and sillimanite (fibrolite); (b) Kyanite porphyroblast with unstable surrounding in mesoscopy scale, the core is kyanite with blue color and surrounding is andalusite with pink color; (c) Kyanite porphyroblast with perfect two cleavages (PPI).

Schistosity	<i>Sn</i> Continuous Foliation	<i>Sn+1</i> Crenulation Cleavage	<i>Sn+2</i> Crenulation Cleavage Local Shear Zone
Deformation	<i>Dn</i>	<i>Dn+1</i> Regional folding	<i>Dn+2</i>
Minerals			
Grt	[Mineral bar]		
St	[Mineral bar]		
Ky	[Mineral bar]		
Sill	[Mineral bar]		
And	[Mineral bar]		
Crd	[Mineral bar]		
Act	[Mineral bar]		
Ms	[Mineral bar]		
Bt	[Mineral bar]		
Metamorphism phases	<i>M1</i> Syn to post <i>Sn</i> Pre <i>Sn+1</i>	<i>M2</i> Post <i>Sn</i> pre <i>Sn+1</i>	
Age(Ma)	~60	younger than <i>M1</i>	

Figure 5. Appearance of metamorphic minerals in relation to different deformational events, timing and metamorphism phases.

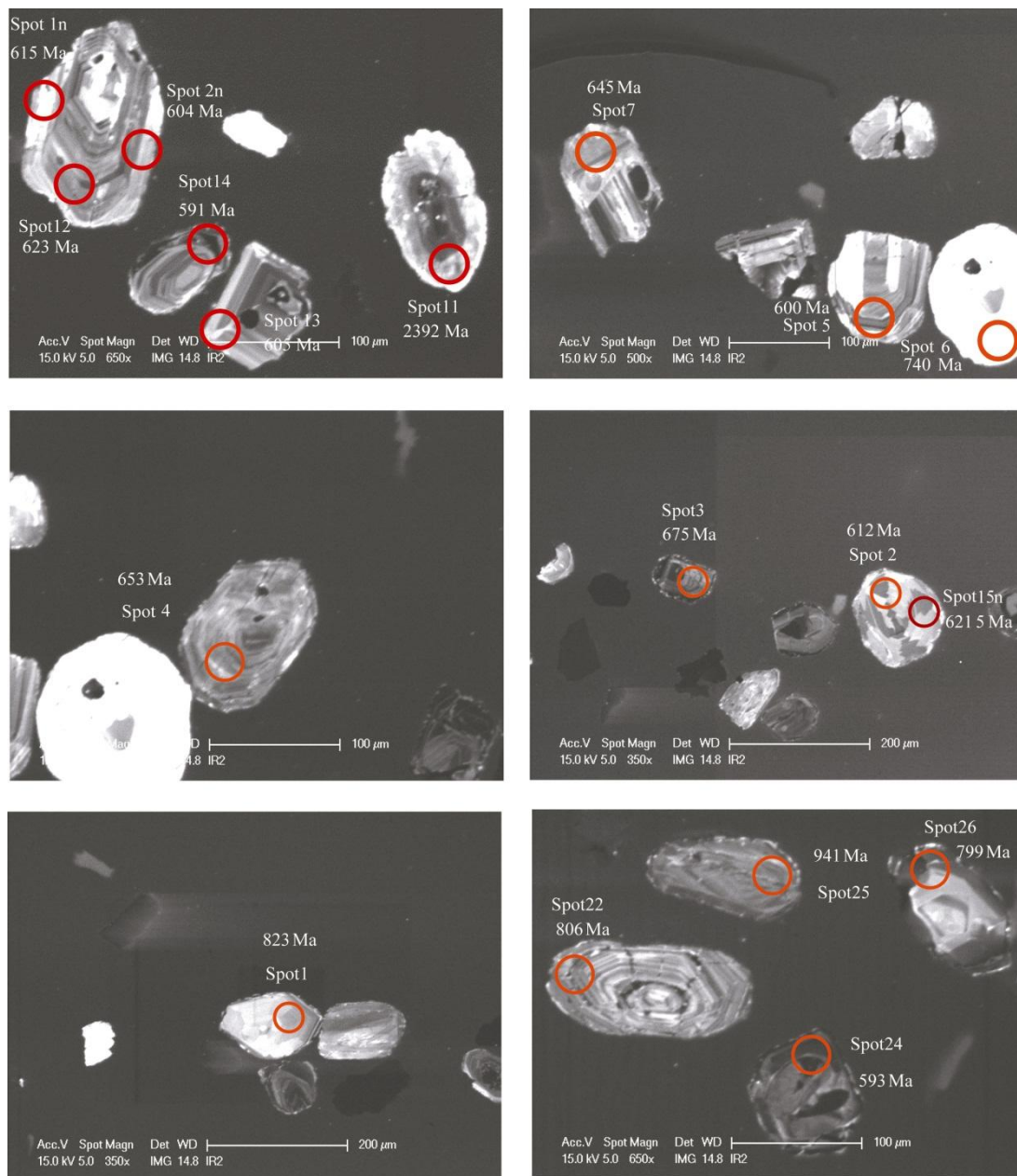


Figure 6. CL images of Zircon analyzed and some analyzed spots from Sh-161.

many parts of SMC (Fig. 2), but assemblage of M2 metamorphic phase is just outcrops close to the quartz porphyry intrusions (Type III), which is represented by porphyritic granite and leucogranite and forms an outcrop in the central part of the complex. A thermal aureole around the Type III intrusions affected the previously regionally metamorphosed schists. The heat of the intrusion was a foundation for the development of andalusite and cordierite in the host metapelitic schists

and actinolite in the host metabasic schists (Fig. 2). Typical Fan types actinolite grow in high T and Low P metamorphism [7, 38] and fan types actinolite in SMC are related to M2 metamorphism (Fig. 3h).

On the basis of a reevaluation and petrography of phase relations in kyanite and andalusite-bearing rocks, Kyanite was first crystallized Al-silicate in SMC. Porphyroblasts of Kyanite with two cleavages are present in core and surrounded by andalusite and

occasionally sillimanite (fibrolite) in mesoscopy and microscopy scales (Fig. 4). Kyanite is unstable with cordierite assemblages and has partially replaced by sillimanite (fibrolite) and andalusite. Recent studies on similar features in metamorphic complexes reported the metastable nature of these parageneses and attributed to presence of two metamorphic stages [25,32,42,53]. Regional folding in SMC occurred after two metamorphic stages (M1, M2), and porphyroblasts show the same petrofabric, but they aren't related to same metamorphic phase and paragenesis [24,30] (Fig. 5).

U – Pb Dating

Age Constraints of Deposition

Sample (Sh-161) from the schists was collected about 2 km east of the village of Qareh Zagh (N36°35'43", E46°52'29") for dating. Metamorphic mineral assemblages of metasedimentary in sample Sh-161 include staurolite, cordierite and andalusite. The sample was collected from a ~2 m-thick outcrop in the central region of SMC. This sample has got M1 staurolite and M2 cordierite, and we tried to obtain two different groups of metamorphic zircons representative for two different metamorphic ages. However, there wasn't any metamorphic zircon (Fig. 6) and their data make up depositional age for the original sedimentary protoliths. It was dated using the LA-ICP-MS at the University of Adelaide. Zircons from this sample are light brown, prismatic, up to 150 µm long, and generally euhedral. CL images show obvious oscillatory zoning (Fig. 6). A weighted mean of the $^{206}\text{Pb}/^{238}\text{U}$ ages from the youngest six >90% concordant analyses produced an age of 605±43 Ma.

This sample contains evidence for a considerable Palaeoproterozoic detrital input into their original sedimentary make up depositional age for the protoliths with constrained age between ~1000 and ~600 Ma (between the youngest reliable detrital zircon and the oldest reliable detrital zircon respectively). With the presented ages, protoliths of metasedimentary rocks of the Soursat Metamorphic Complex are interpreted to be deposited at the same time as the surrounding essentially unmetamorphosed Precambrian-Cambrian sedimentary rocks.

The Age of Metamorphism

Sample Sh-68 was obtained from a ~2 m-thick outcrop of coarse-grained garnet – biotite – quartz metapelitic exposed in northwest of SMC close to the Dowlangaz village. Monazite from this sample was analyzed to determine the time of metamorphism (M1)

from Sn schistosity within the complex. The majority of grains are homogeneous under BSE (Fig. 7). A weighted mean $^{206}\text{Pb}/^{238}\text{U}$ is age of 61±8 Ma obtained.

Metamorphic monazite U–Pb data often show a 1–30 Ma inter- and intra-crystalline age variation (e.g. [8, 11, 12, 19 and 46]). This Variation related to the episodic growth/recrystallisation of monazite during prograde metamorphism. We could accept the age of ~60 Ma as the time of the first metamorphic phase on the SMC.

The Age of Metasedimentary Rocks and Time of their Metamorphism

The presence of Precambrian Iranian basement first reported in Shahin Dezh geological map (scale 1:250000) [2]. The age of 605±43 Ma obtained during this study confirmed that protoliths of SMC formed at the same time as the surrounding unmetamorphosed Precambrian-Cambrian sedimentary rocks. We conclude that the SMC from Iranian block were originally part of a series which named Peri-Gondwanan terranes that reported in different regions in Iran [18,20,37,45,47] and turkey [49].

First metamorphic event in SMC was a regional metamorphism (M1) and occurred later in Paleocene. It could be related to the orogenesis during the collision of Arabian plate with Iranian block and closure of Neotethys.

Based on the dating, protolith of metasedimentary rocks in the SMC are related to the Precambrian-Cambrian. Primary basement rocks metamorphosed because of regional metamorphism (M1) during the Paleocene time.

This activity probably was responsible for exhumation of Neoproterozoic-Early Cambrian basement



Figure 7. Photographs of garnet schist (Sh-68). a) & b) BSE images of monazite analyzed; c) monazite (PPI).

at during the Paleocene time and made M1 metamorphism on Precambrian-Cambrian sedimentary rocks. This event is the same as other metamorphic core complexes in central Iran [51] and Sanandaj-Sirjan metamorphic zone [10, 36] that Verdel [52] related them to the roll-back event in Sanandaj-Sirjan zone.

Second metamorphic stage in SMC is contact metamorphism (M2) that related to the youngest intrusion on complex which its aureole overprinted regional metamorphism (M1).

Acknowledgements

The authors would like to express their gratitude to Angus Netting and Ben Wade of Adelaide Microscopy for assistance with imaging and LAICPMS analysis. ASC and GC's contribution forms TRaX Record #xx. Field sampling financially supported by Research Vice Chancellor of Tarbiat Moallem University.

Reference

- Alavi M. Tectonics of the Zagros orogenic belt of Iran: new data and interpretations. *Tectonophysics*, **229**: 211–238 (1994).
- Alavi M., Hajian J., Amidi A. and Bolurchi H. Gology of Takab-Saein Qaleh: Explanatory note of 1:250000 map of Takab quadrangle, Geological Survey of Iran, Report No.50 (1982).
- Allen M.B. and Armstrong H.A. Arabia-Eurasia collision and the forcing of mid-Cenozoic global cooling. *Palaeogeography, Palaeoclimatology, Palaeoecology*, **265**: 52–58 (2008).
- Allen M.B. Discussion on the Eocene bimodal Piranshahr massif of the Sanadaj_Sirjan Zone, West Iran: a marker of the end of collision in the Zagros orogen. *Journal of the Geological Society, London*, **166**: 981–982 (2009).
- Bea F., Scarrow J.H., Mazhari S.A., Molina J.F., Montero P. S. A. and Ghalamghash J. Reply to discussion on the Eocene bimodal Piranshahr massif of the Sanadaj Sirjan Zone, West Iran: a marker of the end of collision in the Zagros orogen. *Journal of the Geological Society, London*, **166**: 983–984 (2009).
- Berberian M. and King G.C. Towards a paleogeography and tectonics evolution of Iran. *Canadian Journal of Earth Sciences*, **18**: 210–265 (1981).
- Biermann C. Investigations into the development of microstructures in amphibole-bearing rocks from the Seve Koli nappe complex. *PhD Thesis*, Leiden State Univ (1979).
- Bingen B. and van Breemen O. U–Pb monazite ages in amphibolite-to granulite-facies orthogneiss reflect hydrous mineral breakdown reactions: Sveconorwegian Province of SW Norway. *Contrib. Mineral. Petrol*, **132**: 336–353 (1998).
- Darvishzadeh A. *Geology of Iran*, Nashr Emroz publication (in Farsi) (1992).
- Davoudian A. R., Genser J., Dachs E. and Shabanian N. Petrology of eclogites from north of Shahrekord, Sanandaj-Sirjan Zone, Iran. *Mineralogy and Petrology*, **92**: 393–413 (2008).
- Foster G., Kinny P., Prince C., Vance D. and Harris N. The significance of monazite U–Th–Pb age data in metamorphic assemblages: a combined study of monazite and garnet chronometry. *Earth Planet. Sci. Lett*, **181**: 327–340 (2000).
- Foster G.L., Gibson H.D., Parrish R.R., Horstwood, M.S.A., Fraser J. and Tindle, A. Textural, chemical and isotopic insights into the nature and behaviour of metamorphic monazite. *Chem. Geol.* **191**, 183–207 (2002).
- Ghasemi A. and Poor Kerman M. Structure of the Soresat Metamorphic Complex, North Sanandaj-Sirjan Zone, northwest Iran, *Australian Journal of Earth Sciences*, **56**(7): 939–949 (2009).
- Ghasemi A. Structural Study of south Shahin Dezh Metamorphic rocks of NW Iran. *Ph.D.Thesis* (in Farsi), Shahid beheshti university, 117p (2001).
- Guest B., Stockli D.F., Grove M., Axen G.J., Lam P.S., Hassanzadeh J. Thermal histories from the central Alborz Mountains, northern Iran: implications for the spatial and temporal distribution of deformation in northern Iran. *Geological Society of America Bulletin*, **118**: 1507–1521 (2006).
- Haghipour A. Etude géologique de la region de Biabanak-Bafg (Iran Central); petrologie et tectonique du precambrien et de sa couverture. *Ph.D. thesis*, universite scientifique et medicale de Grenoble, France, 403p (1974).
- Haghipour A. Precambrian in central Iran: lithostratigraphy, structural history and petrology. *Iranian Petroleum Institute Bulletin*, **81**: 1–17 (1981).
- Hassanzadeh J., Stockli D. F., Horton B. K., Axen G. J., Stockli L. D., Grove M., Schmitt A. K. and Walker J. D. U–Pb zircon geochronology of late Neoproterozoic–Early Cambrian granitoids in Iran: Implications for paleogeography, magmatism, and exhumation history of Iranian basement. *Tectonophysics*, **451**: 71–96 (2008).
- Hawkins D.P. and Bowring S.A. U–Pb monazite, xenotime, and titanite geochronological constraints on the prograde to post-peak metamorphic thermal history of Paleoproterozoic migmatites from the Grand Canyon, Arizona. *Contrib. Mineral. Petrol*, **134**: 150–169 (1999).
- Horton B.K., Hassanzadeh J., Stockli D.F., Axen G.J., Gillis R.J., Guest B., Amini A., Fakhari M., Zamanzadeh M.S. and Grove G. Detrital zircon provenance of Neoproterozoic to Cenozoic deposits in Iran: Implications for chronostratigraphy and collisional tectonics. *Tectonophysics*, **451**: 97–122 (2008).
- Jackson S.E., Pearson N.J., Griffin W.L. and Belousova E.A. The application of laser ablation-inductively coupled plasma-mass spectrometry to in situ U–Pb zircon geochronology. *Chemical Geology*, **211**(1–2): 47–69 (2004).
- Jamshidi badr M. Petrology and Petrography study of metamorphic and Igneous rocks of Shahin dezah area, *M.S.C. Thesis* (in Farsi), Tabriz university of Iran, 140p (2001).
- Jamshidi badr M., Collins A., Masoudi F. and Mehrabi B. Detrital U–Pb zircon dating of granitoids in the Soresat Complex (NW IRAN). *Geological Society of America Abstracts with Programs*, **41**(7): 113 (2009a).
- Jamshidi badr M., Masoudi. F. and Mohajjel M. State and condition of the formation of cordierite crystal in

- Metapelites of Soursat Complex, *the 17th symposium of Crystallography and Mineralogy of Iran* (2009b).
25. Jessup M. J., Cottle J. M., Searle M. P., Law R. D., Newell D.L., Tracy R. J. and Andwaters D. J. P–T–t–D paths of Everest Series schist, Nepal, *metamorphic Geol*, **26**: 717–739 (2008).
 26. Kholghi khasraghi M.H. and Vossoughi Abedini M. Origin, petrogenesis and radiometric age dating of pichagchi batholite (North West Iran). *Geosci. Iran*, **11**(49-50): 78-89 (2004).
 27. Kholghi khasraghi M.H. Quadrangle Geological Map of Shahin dezh, *Geological Survey of Iran*, scale 1:100,000 (1994).
 28. Macquarie M. Crustal scale geometry of the Zagros fold-thrust belt, Iran. *Journal of Structural Geology*, **26**: 519–535 (2004).
 29. Masoudi. F. and Jamshidi badr M. Biotite and hornblende composition used to investigate the nature and thermobarometry of Pichagchi pluton, Northwest Sanandaj-Sirjan metamorphic belt, Iran. *Journal of Sciences, Islamic Republic of Iran*. **19**(4): 329-338 (2008).
 30. Masoudi. F., Mohajjel M. and Jamshidi badr M. Study of different schistosity in Soursat complex based on distribution of metamorphic minerals, *14th Symposium of Crystallography and Mineralogy of Iran* (2006).
 31. Mazhari S.A. Bea, F. Amini S., Ghalamghash J. Molina J.F., Montero P., Scarrow J.H. and Williams I.S. The Eocene bimodal Piranshahr massif of the Sanandaj-Sirjan Zone, NW Iran: a marker of the end of the collision in the Zagros orogen. *Journal of the Geological Society, London*, **166**: 53-69 (2009).
 32. Mezger M., Passchier C.W. and Régnier J. L. Metastable staurolite-cordierite assemblage of the Bossost dome: Late Variscan decompression and polyphase metamorphism in the Axial Zone of the central Pyrenees. C. R. *Geoscience*, **336**: 827-837 (2004).
 33. Modjarad M. Petrology and geodynamic rocks of sursat (east of Shahin dezh) NW Iran, *Ph.D.Thesis* (in Farsi), Tabriz University, 190p (2007).
 34. Mohajjel M. and Fergusson C.L. Dextral transpression in late Cretaceous continental collision, Sanandaj-Sirjan Zone, Western Iran. *Journal of Structural Geology*, **22**: 1125–1139 (2000).
 35. Mohajjel M., Fergusson C.L. and Sahandi M.R. Cretaceous-Tertiary convergence and continental collision, Sanandaj-Sirjan Zone, western Iran. *J Asian Earth Science*, **21**: 397–412 (2003).
 36. Moritz R. Ghazban F. and Singer B.S. Eocene gold ore formation at Muteh, Sanandaj-Sirjan tectonic zone, western Iran: a result of late-stage extension and exhumation of metamorphic basement rocks within the Zagros orogen. *Economic Geology*, **101**: 1497-1524 (2006).
 37. Nadimi A. Evolution of the central Iranian basement. *Gondwana Research*, **12**(3): 324–333 (2007).
 38. Passchier C.W. and Trouw R.A.J. *Microtectonics*. Springer, 365p (2005).
 39. Payne J. L., Hand M., Barovich K. M. and Wade B. P. Temporal constraints on the timing of high-grade metamorphism in the northern Gawler Craton: implications for assembly of the Australian Proterozoic. *Australian Journal of Earth Sciences*, **55**: 623–640 (2008).
 40. Payne J.L., Barovich K. and Hand M. Provenance of metasedimentary rocks in the northern Gawler Craton, Australia: implications for Palaeoproterozoic reconstructions. *Precambrian Research*, **148**: 275–291 (2006).
 41. Pelissier G. and Blolourchi M. H. East Takab metamorphic Complex. G.S.I. (unpublished) (1967).
 42. R'egnier J. L., Mezger J. E. and Passchier C. W. Metamorphism of Precambrian–Palaeozoic schists of the Menderes core series and contact relationships with Proterozoic orthogneisses of the western C₁ ine Massif, Anatolide belt, western Turkey. *Geol. Mag.* **144**(1): 67–104 (2007).
 43. Ramezani J and Tucker R.D. The Saghand region, central Iran: U-Pb geochronology, petrogenesis and implications for Gondwana tectonics. *American Journal of Science*, **303**: 622-665 (2003).
 44. Sabzehei M. An introduction to general geological features of metamorphic complexes in southern Sanandaj-Sirjan zone. Geological Survey of Iran, (Unpublished, in Persian) (1996).
 45. Saki A. Proto-Tethyan remnants in northwest Iran: Geochemistry of the gneisses and metapelitic rocks. *Gondwana Research*, **17**(4): 704-717 (2010).
 46. Spear F.S. and Parrish R.R. Petrology and cooling rates of the Valhalla complex, British Columbia, *Canadian Journal Petrology*, **37**(4): 733–765 (1996).
 47. Stockli D.F., Hassanzadeh J., Stockli L.D., Axen G.J., Walker J.D. and Dewane T.J. Structural and geochronological evidence for Oligo-Miocene intra-arc low-angle detachment faulting in the Takab–Zanjan area NW Iran. *Geological Society of America Abstracts with Programs*, **36**(5): 319 (2004).
 48. Stocklin J. Structural history and tectonics of Iran: a review. *Am Assoc Petroleum Geol Bull*, **52**: 1229-1258 (1968).
 49. Ustaömer P.A., Ustaömer T., Collins A.S. and Robertson A.H.F. Cadomian (Ediacaran–Cambrian) arc magmatism in the Bitlis Massif, SE Turkey: Magmatism along the developing northern margin of Gondwana. *Tectonophysics*, **473**: 99-112 (2009).
 50. Van Achtenbergh E., Ryan C.G., Jackson S.E. and Griffin W.L. Data reduction software for LA-ICP-MS. In: Sylvester Paul, J. (Ed.), *Laser-Ablation-ICPMS in the Earth Sciences; Principles and Applications*. *Mineralogical Association of Canada*, 239-243 (2001).
 51. Verdel C., Wernicke B.P., Ramezani J., Hassanzadeh J., Renne P.R. and Spell T.L. Geology and thermochronology of Tertiary Cordilleran-style metamorphic core complexes in the Saghand region of central Iran. *Geological Society of America Bulletin*, **119**: 961-977 (2007).
 52. Verdel C. I. Cenozoic geology of iran: an integrated study of extensional tectonics and related volcanism, ii. ediacaran stratigraphy of the north american cordillera: new observations from eastern california and northern Utah, *PhD Thesis*, California Institute of Technology Pasadena, California (2009).
 53. Wei C. J., Clarke G., Tian W. and Qiu L. Transition of metamorphic series from the Kyanite- to andalusite-types in the Altai orogen, Xinjiang, China: Evidence from petrography and calculated KFMASH and KFMASH phase relations. *Lithos*, **96**: 353–374 (2007).